Fermi National Accelerator Laboratory

FERMILAB-Conf-94/044-E

CDF

CDF Electroweak Studies and the Search for the Top Quark

Henry J. Frisch
For the CDF Collaboration

The Enrico Fermi Institute and Physics Department
University of Chicago

Fermi National Accelerator Laboratory
P.O. Box 500, Batavai, Illinois 60510

February 1994

Invited talk at the *XXIII International Symposium on Multiparticle Dynamics,*
Aspen, Colorado, September 14, 1993

Disclaimer

CDF/PUB/ELECTROWEAK/PUBLIC/2404
FERMILAB-CONF-94/044-E

CDF Electroweak Studies and the Search for the Top Quark

Henry J. Frisch
The Enrico Fermi Institute and Physics Department
University of Chicago

For the CDF Collaboration

Abstract

The second major run of the $\bar{p}p$ Fermilab Tevatron Collider ended on May 30. The CDF detector has accumulated almost five times the data sample of its previous 1988-1989 run. We present new results on electroweak physics, including the ratio of W to Z boson production cross-sections, and the charge asymmetry in W decay. We give a progress report on the measurement of the W mass. New results from the 1988-1989 data on $W\gamma$ production are also presented. The status of the search for the top quark in the dilepton modes is described. In addition a status report of the ongoing search in the lepton + jets mode is given.

1 Introduction

On May 30 the Fermilab Tevatron Collider ended Run Ia, which had begun almost a year earlier. Both the CDF and D0 detectors had started taking serious data the previous August. The accelerator delivered 29.9 pb^{-1} [1], more than the goal of 25 pb^{-1}, and CDF recorded 21.4 pb^{-1} of this. Even more impressively, the accelerator hit record luminosities of almost 9×10^{30} cm^{-2} sec^{-1}, with the instantaneous luminosity for the highest luminosity bunch being above 10^{31}. The accelerator will remain off until the late fall; then Run Ib will commence, with a goal of an additional 75 pb^{-1}, and a possible increase in the collision energy from 1.8 TeV to close to 2 TeV. Both D0 and CDF have substantial upgrades in progress for Run II, which follows the Fixed Target run after Collider Run Ib, driven partly by the increased luminosity and by a change in the bunch spacing from 3.5 microseconds to 132 nanoseconds. In the future the Main Injector will allow much higher integrated luminosities, quite possibly many fb^{-1}'s per year.

The results presented here are those preliminary results available at the time of the talk (except where otherwise noted), with most dating from only a few months after the run ended. However there is still too much material to fit in one writeup; in order to do a more complete job on the top quark search status I have shortened the Electroweak section by leaving out the description of new results from the 1988-89 data, in particular the Drell-Yan measurements and some of the $W\gamma$ figures that were presented in the talk, and by abbreviating the other descriptions [2].

Invited talk at the XXIII International Symposium on Multiparticle Dynamics, Aspen Colorado, Sept. 14, 1993

2 W and Z production, R, and the W width

One can extract the width of the W, Γ_W, from the ratio of the W and Z cross-sections times branching ratios, using the method of Cabibbo [3] and Halzen and Mursula [4]. The idea is to compare the ratio of observed $W^{\pm} \rightarrow e^{\pm}\nu$ decays to observed $Z^0 \rightarrow e^+e^-$ decays. The ratio, R, can be expressed as:

$$R = \frac{\sigma(W \rightarrow e\nu)}{\sigma(Z^0 \rightarrow e^+e^-)} = \frac{\sigma(\bar{p}p \rightarrow WX)}{\sigma(\bar{p}p \rightarrow Z^0X)} \frac{\Gamma(W \rightarrow e\nu)}{\Gamma(Z^0 \rightarrow e^+e^-)} \frac{\Gamma(Z^0)}{\Gamma(W)}. \quad (1)$$

From R either the ratio of total widths $\Gamma(Z^0)/\Gamma(W)$ or the branching ratio for W into electrons can be extracted using the predicted value for the ratio of production cross sections, the measured partial and total widths of the Z^0, and the predicted partial widths of the W.

The analysis is based on the same principle as our previous analyses of R [5]: we select a 'good' electron in the central detector where the electron identification is robust, and then select both the W and Z samples as subsets of this inclusive central electron sample. Both the W and Z samples thus share the common first electron leg, and consequently many of the systematic uncertainties involving trigger and electron identification efficiencies cancel. The inclusive sample is selected with electron identification cuts that differ only slightly from those in previous analyses [6]. Figure 1 shows the E_T spectrum of inclusive electrons at this stage of selection.

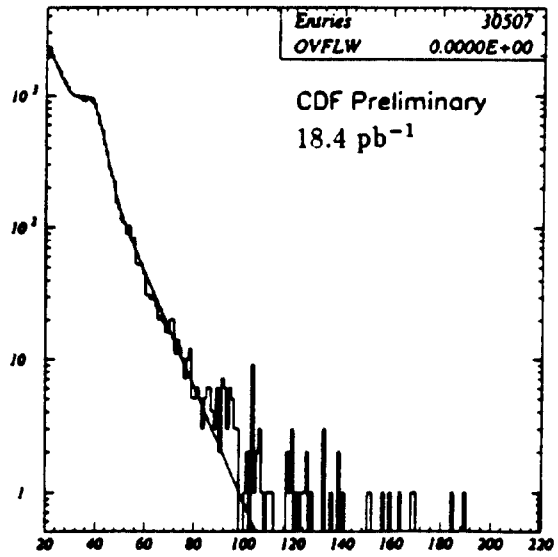

Fig. 1. The E_T spectrum of inclusive electrons. Note the Jacobian peak of the W and Z.

From the inclusive sample W candidates are selected by the requirement of greater than 20 GeV of missing E_T in the event. We select Z candidates by requiring a second electromagnetic isolated cluster in the event which makes an invariant mass with the first electron in the range 65 $GeV/c^2 < M_{ee} <$ 115 GeV/c^2. In 18.4 pb^{-1} there are 30507 inclusive central electrons, 10991 $W^{\pm} \rightarrow e^{\pm}\nu$ candidates, and 1053 $Z^0 \rightarrow e^+e^-$ candidates. Of the Z^0

candidates, 41% are central-central, 49% are central-plug, and 10% are central-forward [7]. The transverse mass spectrum for the W candidates and the invariant mass spectrum for the Z candidates are shown in Figures 2 and 3.

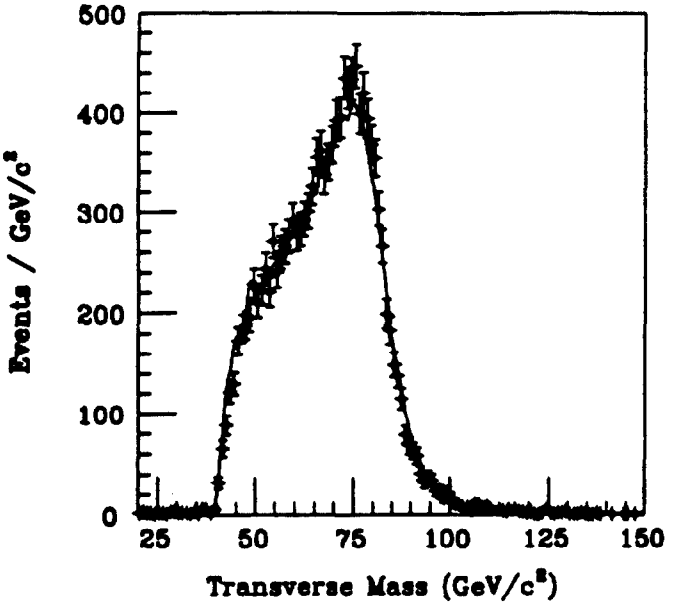

Fig. 2. The W transverse mass spectrum.

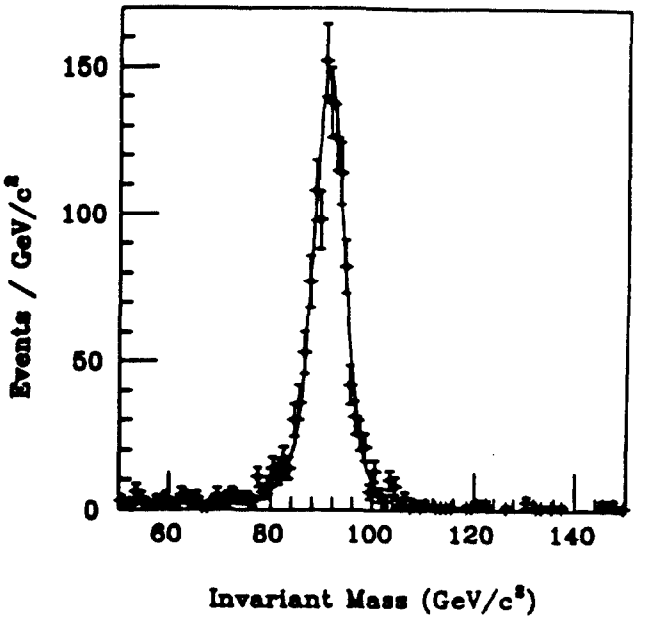

Fig.3. The Z invariant mass spectrum.

The preliminary result for R is:

$$R = 10.65 \pm 0.36(stat.) \pm 0.27(sys.) \tag{2}$$

leading to a value for the inverse of the branching ratio of

$$\Gamma(W \rightarrow e\nu)/\Gamma(W) = 0.1100 \pm 0.0036(stat.) \pm 0.0031(sys.). \tag{3}$$

The preliminary value of $\Gamma(W)$ derived from this is compared to previous measurements and to the Standard Model prediction in Table 1.

This measurement of the branching ratio is sensitive to new decay modes of the W, *e.g.* the W decaying into $t\bar{b}$. The predicted dependence of the branching ratio on the top quark mass is shown in Figure 4, where the inverse of the branching ratio, $\Gamma(W)/\Gamma(W \rightarrow e\nu)$ is plotted versus top mass (the inverse has uncertainties that are more Gaussian). The branching ratio runs from approximately 1/12 to 1/9 as the phase space for the W$\rightarrow t\bar{b}$ channel gets closed. Both the 1-σ and 95% *C.L.* limits from our new measurement are plotted. The result is a decay-mode independent limit on the top mass of $M_{top} > 62\ GeV/c^2$ (95% *C.L.*).

Table 1: Comparison of measurements of the W width

Who	Mode	Reference	W width
CDF	e	PRL 64,152 (1990)	$\Gamma(W) = 2.20 \pm 0.16\ GeV$
CDF	μ	PRL 69,128 (1991)	$\Gamma(W) = 2.21 \pm 0.27\ GeV$
UA1	μ	Phys. Lett. B253,503 (1991)	$\Gamma(W) = 2.19 \pm 0.30\ GeV$
UA2	e	Phys. Lett. B276,365 (1991)	$\Gamma(W) = 2.10 \pm 0.16\ GeV$
CDF	e	Preliminary 1993	$\Gamma(W) = 2.033 \pm 0.09\ GeV$
St. Mod.	e,μ	Ref. [8]	$\Gamma(W) = 2.067 \pm 0.021\ GeV$

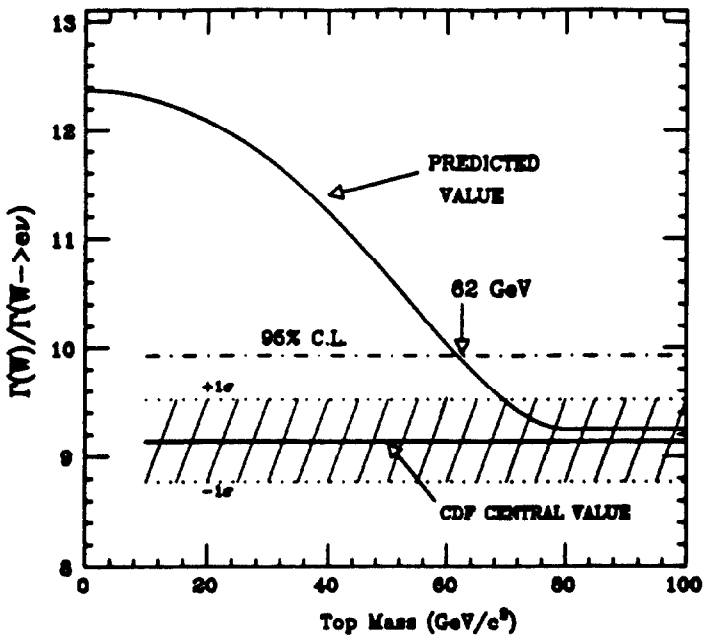

Fig.4. The predicted dependence of the inverse of the branching ratio, $\Gamma(W)/\Gamma(W \to e\nu)$, as a function of top mass. The preliminary results from CDF are shown, with both the 68% and 95% confidence limits.

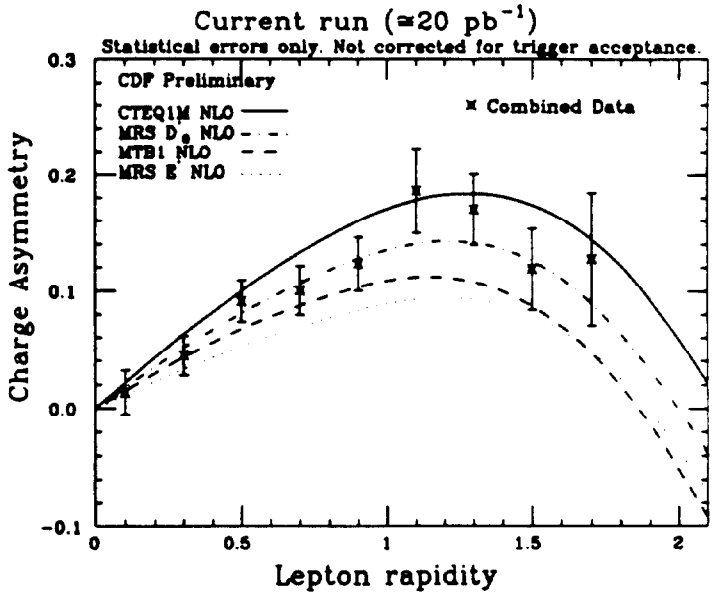

Fig. 5. Preliminary results on the forward-backward charge asymmetry versus lepton rapidity.

3 The Forward/Backward Charge Asymmetry in W decay

In $\bar{p}p$ collisions at $\sqrt{s} = 1.8$ TeV approximately 85% of the W bosons are produced in valence-valence or valence-sea collisions [10] leading to a forward-backward charge asymmetry with W^+'s boosted on average in the proton (forward) direction. A second, competing (in sign) source is the V-A decay of the W. The V-A decay gives a lepton angular distribution which tosses the lepton *backward*. The relative size of these two competing effects in the asymmetry is dependent on the selection cuts, as well as $\sqrt{s}$. For our cuts, which select electrons at high

p_T and hence preferentially select decays in which the lepton emerges at 90° from the beam directions, and at $\sqrt{s} = 1.8\ TeV$, the production effect is dominant. The measurement is in fact not very sensitive as a test of V-A, but measures the u and d parton distributions.

For this measurement,where the determination of the lepton sign is necessary, the maximum rapidity is restricted to $|\eta| < 1.7$. Figure 5 shows new preliminary results on the charge asymmetry versus lepton rapidity. We also show the predictions of recent structure functions, and one not-so-recent (MRSE) just to demonstrate that something does not fit well. The agreement with MRSD0, for example, is excellent.

4 The W Mass Measurement

At present the W mass is known to 270 MeV/c^2 from the measurement of $M_W = 80.35 \pm 0.37$ GeV/c^2 by UA2 [11] and the measurement of $M_W = 79.91 \pm 0.39$ GeV/c^2 by CDF [12]. The world average is then $M_W = 80.14 \pm 0.27$ GeV/c^2 .

The analysis of the data from the 1992-93 run is well underway. There is approximately five times the data as from the 1988-89 run. We determine the mass from the transverse mass distribution formed from the electron p_T and the missing Et observed in the detector. The electron p_T depends on calibrating the magnetic spectrometer and the central electromagnetic calorimeter. The calibration of the electromagnetic calorimeter is done *in situ* using the measured momentum of electrons above 9 GeV to balance the electromagnetic towers of the calorimeter, and using the momentum of electrons from W decay for the overall calibration. We are thus using the magnetic spectrometer to calibrate the calorimeter in an absolute fashion. Figure 6 shows the spectrum in E/p, where E is the calorimeter response and p is the measured momentum from the track, for electrons from W decay. Also shown is the prediction from a Monte Carlo that includes radiation. The radiative tail matches the data well. Figure 7 shows the reconstructed Z peak and the Monte Carlo prediction. The Z mass peak is not used in the normalization of the W mass, but is used only as a check; this is thus not a measurement of M_W over M_Z, but of M_W. As long as CDF is in this regime where the statistics dominate both the statistical and systematic errors we do better with the direct measurement than by normalizing to the Z mass due to the limited statistics on the Z.

The larger data sample from the new run allows a new strategy for the W mass analysis. The transverse mass can be approximated by:

$$M_T \cong 2P_T^{lepton} + u_{parallel}, \tag{4}$$

where $u_{parallel}$ is the component along the lepton direction of the transverse energy recoiling against the W. The new wrinkle is measuring the detector response to the recoil energy by using $Z^0 \rightarrow e^+e^-$ decays where both u and and the p_T of the Z can be measured. This leads to a modelling of the detector response where there are no tunable detector parameters, and only the input W Pt spectrum can be varied (within experimental limits). This is one example of how the larger statistics from runs with increasing luminosity allows a beating down of the systematic uncertainties as well.

At the time of the talk a preliminary number on the W mass measurement was not available. Since then, a preliminary number for the electron decay mode has been presented [13]. The measurement in the muon mode is also well underway.

How well will we be able to do on the W mass measurement in the future? We are at present in a regime where the overall uncertainty on the W mass scales approximately as the square root of the number of events, as both the systematic and statistical uncertainties are improving with more data.

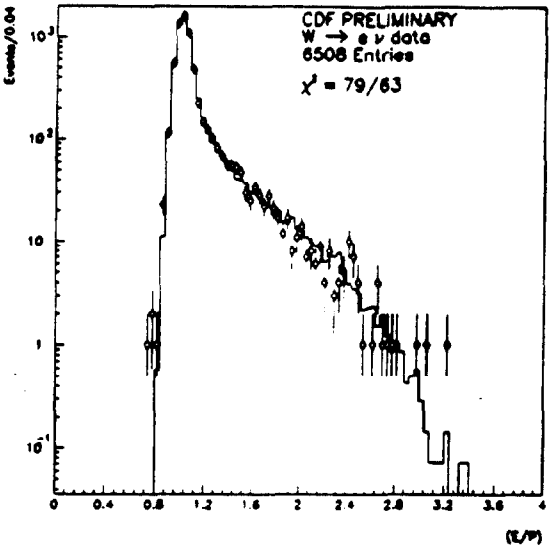

Fig.6. The distribution of E/p, where E is the calorimeter energy and p is the track momentum, for electrons from W decay. The curve is the prediction of a radiative Monte Carlo.

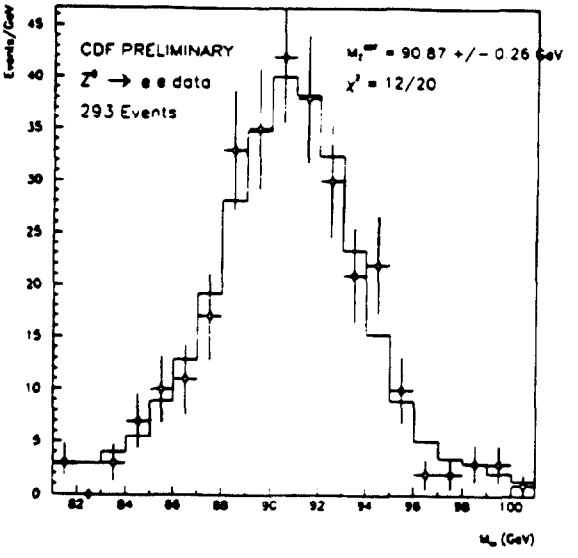

Fig. 7. The measured $Z^0 \rightarrow e^+e^-$ mass spectrum. The normalization is determined from E/p and is absolute. The solid line is the prediction of the Monte Carlo.

One can thus define a figure of merit for a given detector that characterizes the power of the measurement. One such (crude– not all events have equal weight in the mass measurement) figure of merit is the number of W events per pb^{-1} used in the measurement. Another measure is statistical error times the square root of the number of events: this characterizes the power per event. Finally, the statistical error times the square root of the integrated luminosity characterizes both the acceptance (and in the case of UA2, the production cross-section) and the resolution. Table 2 shows these measures for both the published UA2 and CDF measurements, and shows the number of events that have been presented in preliminary fashion by D0 [14] and CDF [2] for the new data. The last entries are recent, and consequently there are many blanks to be filled in.

At present all uncertainties in the CDF measurement are still scaling approximately with the inverse of the square root of the luminosity (*i.e.* statistics). Figure 8 shows the uncertainty on the W mass *if* this dependence continues. Figure 9 shows the breakdown of the uncertainties from the 1988-89 analysis. The big contributions to the systematic uncertainty are in the categories of Parallel Balance and Resolution and W Pt, each of which is measured from the data, and whose contributions will decrease with statistics. After Run Ib, for which

Table 2: Comparison of existing measurements of the W mass

Who	l	L pb^{-1}	Evts	σ_{stat} MeV	σ_{sys} MeV	σ_{tot} MeV	$\sigma_{stat} \times \sqrt{L}$ MeV/$(pb)^{-1/2}$	$\sigma_{stat} \times \sqrt{Ev}$ GeV	Ev/pb^{-1} $/pb^{-1}$
CDF	e	4.4	1130	350	240	465	692	11.8 ± 0.4	257
CDF	μ	3.9	592	530	315	620	1046	12.9 ± 0.5	152
UA2	e	13.0	2065	330	170	370	1190	15.0 ± 0.3	159
1992-1993 Results									
D0	e	14.8	8182						553
CDF	e	19	6974						367
CDF	μ	21	5650						269

the goal is 75 pb^{-1}, if no new systematic uncertainties appear one could hope for an overall uncertainty on M_W of close to 100 MeV. Below this level the ultimate sensitivity is unknown: the number of 50 MeV is bandied about, but cannot yet be taken seriously as either possible or impossible. However if both D0 and CDF could reach the 50 MeV level with 1 fb^{-1}, the combined number from Fermilab would reach 35 MeV.

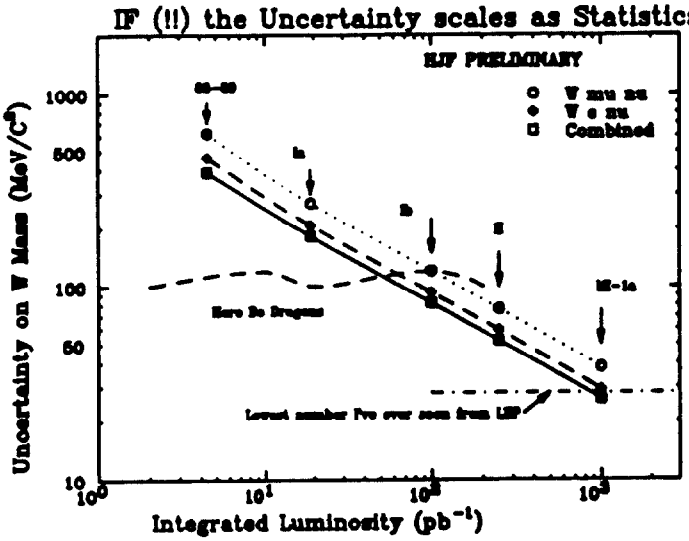

Fig.8. The uncertainty on the W mass, from the CDF electron, muon, and combined analyses, versus integrated luminosity, assuming that the systematic uncertainties continue scaling with statistics.

Uncertainty	Electrons	Muons	Common
Statistical	350 (440)	530 (650)	
Energy scale	190	80	80
(1) Tracking chamber	80	80	80
(2) Calorimeter	175		
Systematics	240	315	150
(1) Proton structure	60	60	60
(2) Resolution, W p_T	145	150	130
(3) Parallel balance	170	240	
(4) Background	50	110	
(5) Fitting	50	50	50
Overall	465 (540)	620 (725)	

Fig. 9. The contributions to the W mass uncertainty from the 1988-89 analysis [12].

One can compare this with projections for LEP200 assuming a beam energy of 88 GeV and an integrated luminosity of 500 pb^{-1}, which could occur in 1998 after 3 years of running [15]. From direct reconstruction LEP estimates an uncertainty per experiment of 55 MeV, from the excitation curve an uncertainty of 100 MeV, and from the lepton end-point

an uncertainty of 150 MeV. Combining all four LEP experiments and a lot of optimism they estimate the direct reconstruction could give a statistical error of 28 MeV and a systematic error of 24 MeV. One really doesn't know what systematic problems one will run into at these levels at D0 and CDF, and the only conclusion I can draw is that at least on paper Fermilab and LEP200 are competitive.

5 Wγ, $Z\gamma$ WW and WZ Pair Production

The production of boson pairs tests the triboson gauge couplings; new results are available from the 1988-89 data. The number of events observed and the expectations are given in Table 3. From these one can extract the values of the parameters $\Delta\kappa$ and λ, which are related to the magnetic dipole and electric quadrupole moments by $\mu_W = \frac{e}{2M_W}(2 + \Delta\kappa + \lambda)$ and $Q_W = -\frac{e}{M_W^2}(1 + \Delta\kappa - \lambda)$, respectively.

These limits are given in Table 4. The reader is referred to the talk by Muller [2]for a fuller discussion. Results from the 1992-93 data should be available soon.

Table 3: Summary of $W\gamma$ and $Z^0\gamma$ Results

Channel	N_{obs}	$\sum N_{bkgnd}$	N_{signal}	N_{pred}^{SM}
$e\ W\gamma$	8	$3.8 \pm 0.8 \pm 1.5$	$4.2 \pm 2.9 \pm 1.5$	4.6 ± 0.4
$\mu\ W\gamma$	5	$2.3 \pm 0.4 \pm 0.9$	$2.7 \pm 2.3 \pm 0.9$	2.5 ± 0.2
$e\ Z^0\gamma$	2	$0.3 \pm 0.1 \pm 0.1$	$1.7 \pm 1.4 \pm 0.1$	1.2 ± 0.1
$\mu\ Z^0\gamma$	2	$0.1 \pm 0.1 \pm 0.1$	$1.9 \pm 1.4 \pm 0.1$	0.7 ± 0.1

The production of WW and WZ pairs tests the gauge couplings as well, although the cross-sections are smaller, and in the most obvious analyses one pays the price for leptonic branching ratios that do not exist in the $W\gamma$ and $Z^0\gamma$ case. Typical predicted cross-sections [16] are small, 6.7 *pb* for WW production, and 1.7 *pb* for $ZW^+ + ZW^-$ production. Note that these do not include branching ratios, which are of order 3% for $Z^0 \rightarrow e^+e^-$ and 10% for $W^\pm \rightarrow e^\pm\nu$, leading to an expectation of 0.1 WZ events in our sample. Such events, however, are quite striking. Figure 10 shows a CDF event with three high-Pt electrons and missing Et. Two of the electrons make a system with the invariant mass of the Z, and the third when combined with the missing Et gives the transverse mass of the W. The event is 'typical', in that it is the only such one we have. We hope for many more in the upcoming runs.

Table 4: $e + \mu$ Combined $W\gamma$ $\Delta\kappa$ $-$ λ Limits

Parameter	CL Range	$e + \mu$ Limits
$\Delta\kappa$	68.3% *DS CL*	$0.0^{+4.7}_{-4.2}(stat) \pm 0.6(syst) = 0.0^{+5.3}_{-4.8}(stat + syst)$
	68.3% *SS CL*	$-3.2 < \Delta\kappa < +3.7$
($\lambda = 0$)	90.0% *SS CL*	$-5.7 < \Delta\kappa < +6.1$
	95.0% *SS CL*	$-6.5 < \Delta\kappa < +7.0$
λ	68.3% *DS CL*	$0.0^{+2.0}_{-2.0}(stat) \pm 0.3(syst) = 0.0^{+2.3}_{-2.4}(stat + syst)$
	68.3% *SS CL*	$-1.6 < \lambda < +1.6$
($\Delta\kappa = 0$)	90.0% *SS CL*	$-2.7 < \lambda < +2.7$
	95.0% *SS CL*	$-3.1 < \lambda < +3.1$

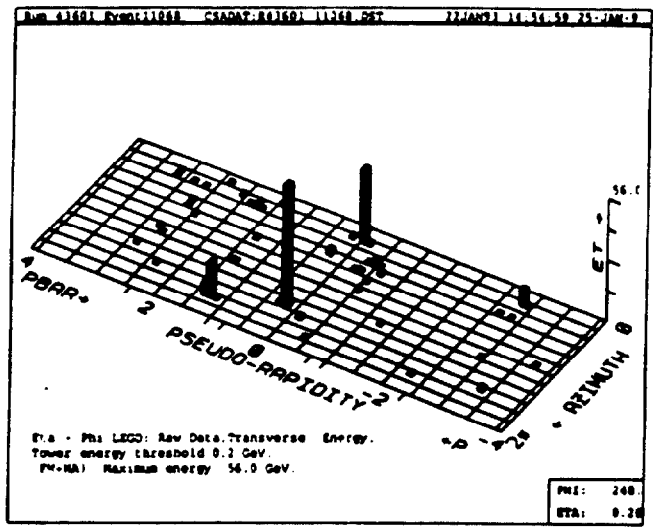

Fig.10a.The Lego plot for a three-electron event. The invariant mass of one oppositely-charged pair is the Z mass, and the transverse mass of the remaining electron with the missing momentum is consistent with a W.

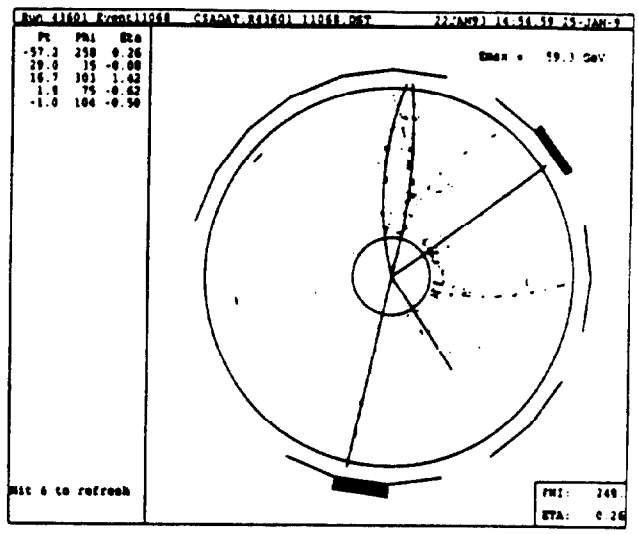

Fig. 10b. The Central Tracking Chamber r-ϕ view of the same event.

6 Search for the Top Quark

We are quite sure the top quark exists from measurements of the isospin of the b quark [17] that show the b quark is the lower component of an isospin doublet, and measurements of the hadronic width of the Z to $b\bar{b}$ find a width of $\Gamma_{b\bar{b}}$= 383 $\pm$ 49 MeV, compared to the

prediction of 24 MeV for an isosinglet b and of 376 MeV for an isodoublet [18]. What is interesting is that the top quark is so heavy- heavier than the electroweak gauge bosons, and much heavier than the other quarks or leptons. The large mass leads to two aspects of the interest - one is that the mass is the most important unknown parameter at present in the precision game of testing the consistency of the Standard Model [19]. The second aspect, to me the more interesting one, is that the top quark's being so heavy may have a deeper significance [20].

The global fits to electroweak data allow an indirect determination of the top quark mass from its contributions to radiative corrections [21]. However if one is hard-nosed about using 95% C.L. limits on the mass, there is still available a wide range in possible mass. Figure 11 shows the best fit predictions to the top mass from 1992 to the present [22]

The direct searches I will describe here put a preliminary limit of $M_T > 113\ GeV/c^2$, from the dilepton modes, adding in 21.4 pb^{-1} of the 92-93 data to 4.4 pb^{-1} of the 1988-89 data. The limits I will describe here are as of the Lepton-Photon conference (August, 1993); the cuts and event selections, however, are the canonical numbers as of the writing of the talk [23]. The analysis presented here is very preliminary, being a 'snapshot' taken only two months after data taking finished, and one that relies on a new detector component (the silicon tracker) and new techniques, particularly in background estimation.

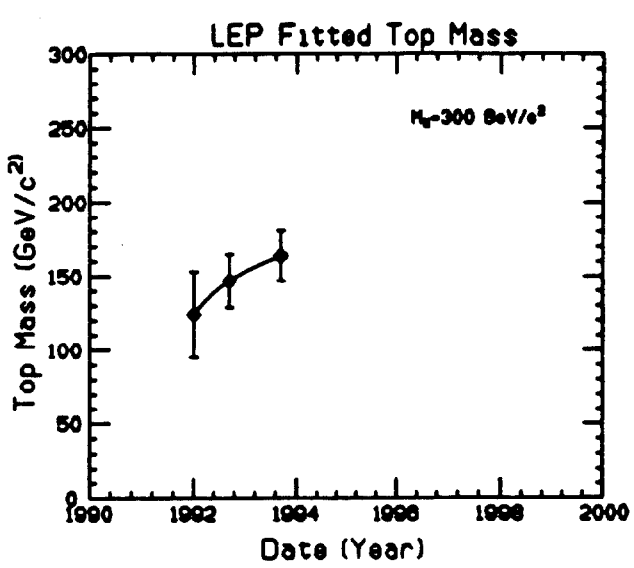

Fig.11. The predicted top mass from the global LEP fits vs time [22].

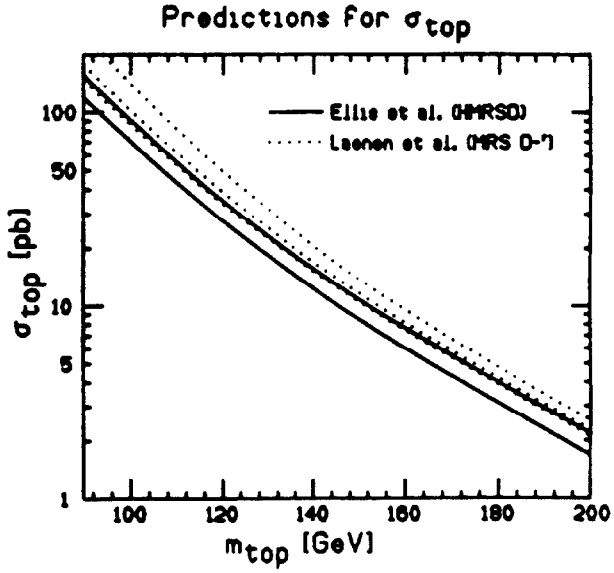

Fig.12. The LO (solid) [25] and NLO [26] predicted cross-sections for top quark pair production. The solid lines show the central value and a lower 1σ limit, and the dotted show the central value and 1σ upper and lower limits.

The predicted cross-sections for the production of top are shown in Figure 12. Both leading order predictions of Ellis *et al.* [25] and NLO predictions of Laenen *et al.* [26] are shown. CDF has used the the lower limit of the LO calculation in its limit to be conservative; it is easy to read off of the plot the limit obtained by using other curves [24]. Figure 13a

shows the relative contribution of $q\bar{q}$ and gg diagrams to the NLO cross-section [26], and 13b shows the 'K-factor' for gg, $q\bar{q}$, and the total of qg, $\bar{q}g$, $q\bar{q}$ and gg. One sees that the glue-glue contribution has a large (and hence uncertain, as this is only the next order) correction.

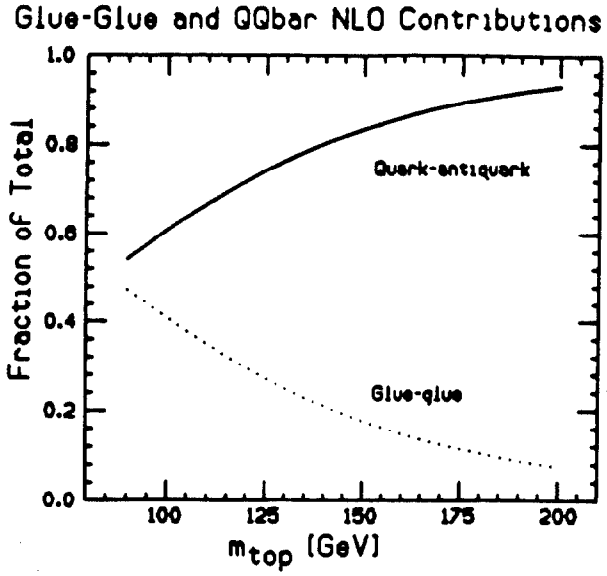

Fig.13a.The relative contribution of $q\bar{q}$ and gg diagrams to the NLO cross-section (from Laenen).

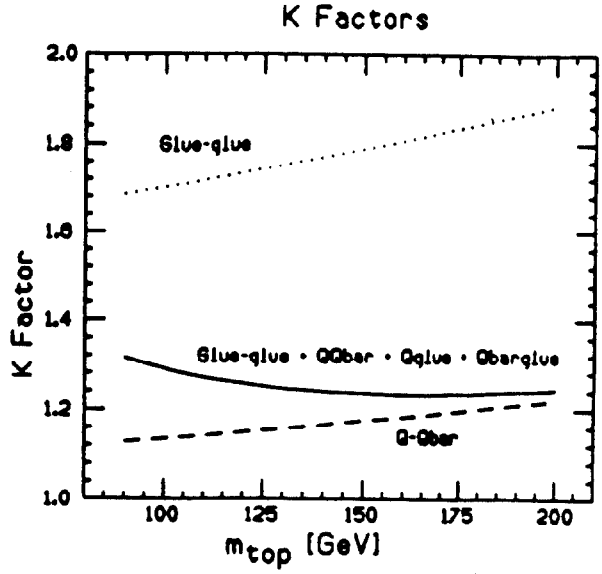

Fig. 13b. The 'K-factor' for gg, $q\bar{q}$, and the total of qg, $\bar{q}g$, $q\bar{q}$ and gg (from Laenen).

The signatures of top production are summarized in Figure 14. We are searching for the production of a $t\bar{t}$ pair (the production of a single top via a virtual W is expected to be much lower). Both tops are expected to decay entirely into Wb, leading to a final state with 2 W's and a b and a $\bar{b}$. The W's decay equally into each of the 9 weak isodoublet pairs (the 3 lepton pairs and 3 colors $\times$ the two quark doublets that are lighter than the W), leading to the matrix of final states from the W's shown in Figure 14. The cleanest modes are the ones where both W's decay into $e\nu$ or $\mu\nu$, leaving us with two high p_T leptons, missing E_T, and 2 jets which are b's, but the total branching ratio is only 4/81. The next cleanest are where one of the 2 W's decays into $e\nu$ or $\mu\nu$, and the other decays into $c\bar{s}$ or $u\bar{d}$, leading to one high p_T lepton, missing E_T, and 4 jets, of which 2 are b's. The total branching ratio for this is 24/81. Finally, there are the τ modes, and the all-hadronic mode, with 6 jets. These are challenging, and are being worked on, but will not be discussed here.

6.1 The Dilepton Analysis

The dilepton analysis selects two high p_T leptons, either muon or electron. It is an analysis that is intended to pick out the modes in Figure 14 where both W's decay leptonically, although for higher top masses it sees a contribution of up to about 7% from the case where one lepton comes from a W and the other from the decay chain of one of the b quarks.

The selection asks for 2 leptons with transverse momentum above 20 GeV, missing Et ($\not\!\!E_T$) greater than 25 GeV, and 2 jets with E_T above 10 GeV. The jet energies used are the uncorrected observed cluster energies, and thus are typically $20 - 40\%$ lower than the original parton energy. In addition, one lepton is always required to be isolated, and for some topologies both are (see below).

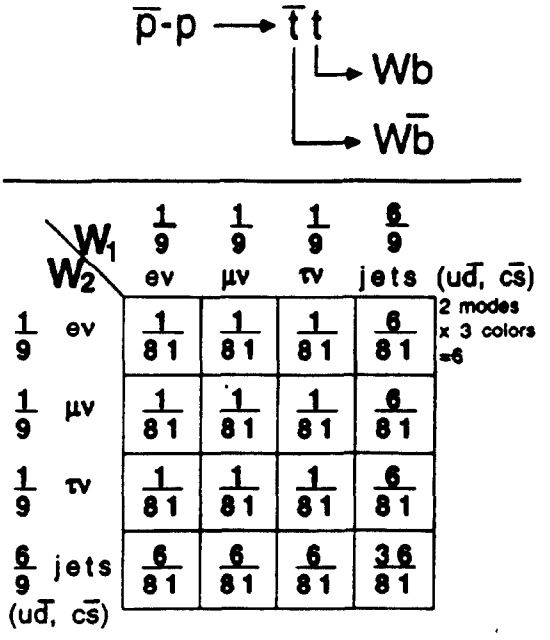

Fig.14. The signatures resulting from top pair production, and the branching ratio matrix resulting from the decay of the 2 W bosons. The final signatures are the sum of the 2 b jets and the decay products listed in the matrices.

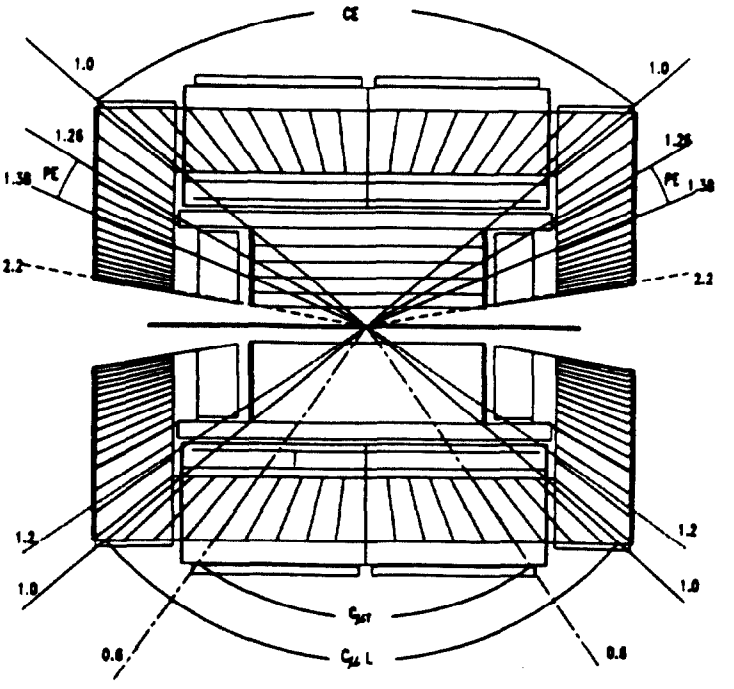

Fig.15. A side view of the detector showing the rapidity range of the three electron categories for the dilepton analysis (top half of the figure), and of the three muon categories (bottom half).

In an effort to increase the acceptance and efficiency for the leptons, the analysis has defined 6 categories of leptons, 3 for electrons and 3 for muons. There are 'tight' and 'loose' central electrons, and also 'plug' electrons. Figure 15 shows the rapidity (η) range of these in the detector. For muons there are also 'tight' and 'loose' central categories, and an even looser category where muons are identified without use of muon chambers at all by identifying high momentum tracks pointing into the fiducial volume of the calorimeter that deposit energy consistent with a charged particle traversing the calorimeter without interacting (often loosely called 'minimum ionizing'). The rapidity ranges for these three categories are also shown in Figure 15.

The selection cuts for each of the six categories are given in Table 5. Most of these cuts are relatively standard lepton identification cuts, and are described in previous publications [27]. To be complete, a glossary of the cut variables is provided in Table 6.

With the six single lepton categories, one can form 21 different dilepton categories, as shown in Figure 16. CE_T and CE_L are tight and loose central electron, respectively. PE^{iso} is an isolated electron in the plug. $C\mu_T$ and $C\mu_L$ are tight and loose central muon, respectively. μ^{iso}_{MI} is an isolated calorimeter muon. Of these 16, we use 12, indicated with the check marks in Figure 16. At least one lepton is required to be in the CE, MU, or MI categories, and is required to pass the track isolation cut (Σ (p_T in a cone of R=0.25) < 3 GeV/c). In addition, plug electrons and calorimeter muons are always required to pass the calorimeter isolation cut of $Iso < 0.1$ in a cone of radius 0.4 around the lepton.

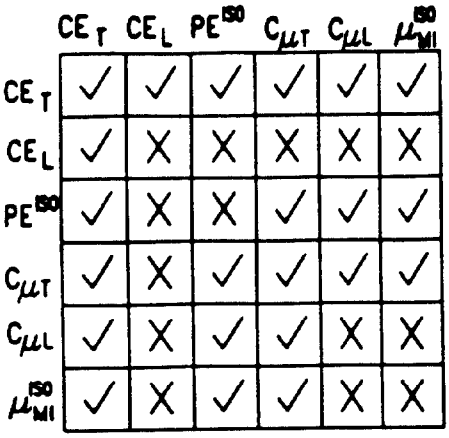

Fig.16. The matrix of categories used in the dilepton analysis (see text).

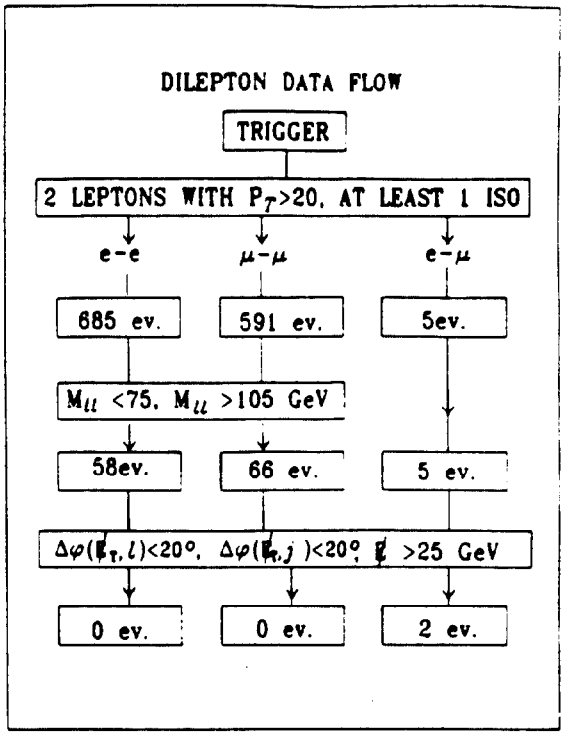

Fig.17. The event selection data flow for the dilepton analysis.

Table 5: Cuts for the electron and muon lepton categories.

Tight Central Electrons			Loose Central Electrons			Plug Electrons		
E_t	>	20 *GeV*	E_t	>	20 *GeV*	E_t	>	20 *GeV*
P_t	>	10 *GeV/c*	P_t	>	10 *GeV/c*	P_t	–	–
E/p	<	2.0	E/p	<	4.0	E/p	–	–
Had/EM	<	0.05	*Had/EM*	<	$.055 + .045E_t/100$	*Had/EM*	<	0.05
Lshr	<	0.2	*Lshr*	<	0.2			
Δx	<	1.5 cm	Δx	<	1.5 cm			
Δz	<	3.0 cm	Δz	<	3.0 cm			
χ^2(*strip*)	<	15	–	–	–			
						$\chi^2(3 \times 3)$	<	3
						χ^2(*depth*)	<	15
						VTX occup.	>	50%
						3Dtrack		
						AxialSLs	≥	3
						Isol.	<	0.1
						TrackIsol	=	0 tracks
Tight Central Muons			**Loose Central Muons**			**Calorimeter Muons**		
P_t	>	20 *GeV/c*	P_t	>	20 *GeV/c*	P_t	>	20 *GeV/c*
EM	<	2 *GeV*	*EM*	<	2 *GeV*	*EM*	<	2 *GeV*
HAD	<	6 *GeV*	*HAD*	<	6 *GeV*	*HAD*	<	6 *GeV*
EM + HAD	>	0.1 *GeV*	*EM + HAD*	>	0.1 *GeV*	*EM + HAD*	>	0.1 *GeV*
d_0	<	3 mm	d_0	<	3 mm	d_0	<	3 mm
Δz_{vert}	<	5 cm	Δz_{vert}	<	5 cm	Δz_{vert}	<	5 cm
Δx(*CMU*)	<	10 cm	Δx(*CMU*)	<	10 cm	Δx(*CMU*)	–	–
Δx(*CMUP*)	<	20 cm	Δx(*CMUP*)	<	20 cm	Δx(*CMUP*)	–	–
Δx(*CMUX*)	–	–	Δx(*CMUX*)	<	20 cm	Δx(*CMUX*)	–	–
AxialSLs	≥	3	*AxialSLs*	≥	3	*AxialSLs*	≥	3
StereoSLs	≥	2	*StereoSLs*	≥	2	*StereoSLs*	≥	2
TotalSLs	≥	6	*TotalSLs*	≥	6	*TotalSLs*	≥	6
						Isol.	<	5 *GeV*

Table 6: A glossary of the cut variables for the electron and muon lepton categories.

All Electrons	
E_t	Transverse Energy of the electron as measured by the calorimeter
P_t	Transverse Momentum of the electron as measured by the tracking
E/p	Ratio of calorimeter energy to track momentum of the electron
Had/EM	Ratio of hadronic to electromagnetic energy in the electron cluster
Central Electrons	
$Lshr$	Lateral shape chisquare for energy sharing in calorimeter towers
$\chi^2(strip)$	Lateral shape chisquare for shape in the shower max chamber
Δx	Matching transverse error between projected track and shower max cluster
Δz	Matching transverse error between projected track and shower max cluster
Plug Electrons	
$\chi^2(3 \times 3)$	Lateral shape chisquare for energy sharing in calorimeter towers
$\chi^2(depth)$	Longit. shape chisquare for energy sharing in calorimeter towers
VTX occup.	Ratio of observed to expected hits in the Vertex Chamber
$Isol.$	Calorimeter energy in a cone of radius R=0.4 around electron (excluding the electron energy E_t) divided by E_t
$Track\ Isol$	No additional track with $Pt > 1.5\ GeV/c^2$ in a cone of R=0.25 around electron
$Axial\ SLs$	The number of axial layers used in the electron track
All Muons	
P_t	Transverse Momentum of the muon as measured by the tracking
EM	Energy deposited in the electromagnetic calorimeter by the muon
HAD	Energy deposited in the hadronic calorimeter by the muon
d_0	Impact parameter of track with the beam line (for this the track is not beam-constrained, and the beamline position is corrected run-by-run)
Δz_{vert}	Matching error between track and a primary vertex
$\Delta x(CMU)$	Matching error between projected track and central muon chamber stub
$\Delta x(CMUP)$	Matching error between projected track and upgrade muon chamber stub
$\Delta x(CMUX)$	Matching error between projected track and extension muon chamber stub
$Isol.$	Calorimeter energy in a cone of radius R=0.4 around muon (excluding the energy deposited by the muon) Note- NOT a ratio
$Axial\ SLs$	The number of axial layers used in the muon track
$Stereo\ SLs$	The number of stereo layers used in the muon track
$Total\ SLs$	The total number of layers used in the muon track

The event selection statistics are shown in Figure 17. First we require two leptons with $p_T > 20$ GeV/c. We then ask that the leptons be of opposite sign (this is expected to remove about 6% of the top signal, but suppresses backgrounds by a much larger amount). A large background in the e-e and $\mu - \mu$ channels comes from the Z: we remove events with dilepton invariant mass between 75 and 105 GeV/c^2 in these two channels. The requirement of $\not\!\!E_T$ greater than 25 GeV leaves 2 $e\mu$ events and one $\mu\mu$ event at this stage. We then apply a cut on the direction of the missing E_T vector requiring that it point at least 20° from the direction of either lepton or any countable jet (see below) in the event. This discriminates against leptons from τ or heavy flavor decays, and against missing E_T due to mis-measured jets. This cut is applied only for events with a total missing E_T less than 50 GeV. Lastly, to suppress WW, WZ and $Z \rightarrow \tau\tau$ background for high mass top, we require two jets with $E_T > 10$ GeV (raw energy) and $|\eta| < 2.4$ be present in the event. The efficiency of this cut is predicted using ISAJET to be 63% for a 120 GeV top, rising to 84% for a 160 GeV top. The two $e\mu$ events alone survive these final cuts.

The efficiency of these categories (summed over tight and loose for both e and μ) is shown in Figure 18, along with the number of events expected in 21.4 pb^{-1} for a top mass of 140 GeV. The efficiencies are the percentages of 4/81 (the branching ratio to e and μ modes) that we accept (there is a subtlety in that one of the leptons can in fact come from a b or τ decay and not from a W, so the 'efficiency' can in fact be greater than 100%.)

NUMBER OF EVENTS EXPECTED
IN 21.4 pb^{-1} (MT=140 GeV)

	CE	PE	MU	MI
CE	0.40 2.4%	0.03 0.2%	1.02 6.2%	0.20 1.2%
PE			0.06 0.3%	0.01 .1%
MU			0.35 2.1%	0.10 0.6%
MI				

EFFICIENCY (%)NORMALIZED TO 4/81

Fig.18. The efficiencies for the central electron (CE=summed over tight and loose), plug electron (PE), central muon (CM=summed over tight and loose), and calorimeter muon (MI).

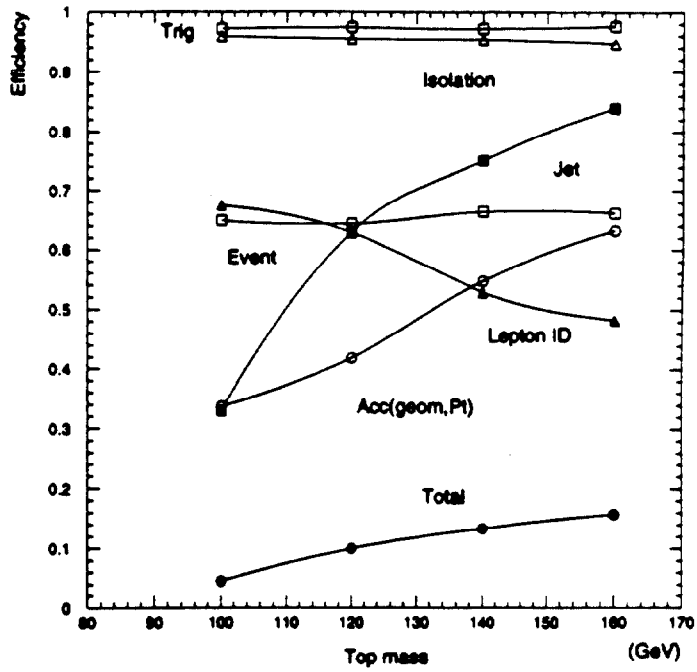

Fig.19. The detection efficiency for top to dileptons, normalized such that 1 is 4/81 of all top decays (the branching ratio for both W's to either e or μ).

The detection efficiencies averaged over these categories are shown in Figure 19 versus top mass. The total efficiency is a product of: 1) the trigger efficiency, 2) the efficiency of the isolation cuts, 3) the 2-jet requirement, 4) the missing Et, jet- and lepton- missing Et angle cuts, the Z mass cut, and the jet pt cuts (labelled 'Event' in the figure), 5) an acceptance (labelled Acc(geom and Pt) in the figure) that includes the fiducial volume cuts and the lepton pt cuts, and 6) the lepton identification cuts. The total efficiency rises with top mass from 4.4% for a top mass of 100 GeV to 15.4% at a top mass of 160 GeV, largely because of increased acceptance for the 2 jets.

Figure 20 shows the distribution of events in the $\not\!\!E_T$ versus $\Delta\phi$ ($\not\!\!E_T$,jet or lepton) plane for ee and $\mu\mu$ events that survive the invariant mass cut, and for the e-μ events, where $\Delta\phi$ ($\not\!\!E_T$,jet or lepton) is the angle between the missing Et and the closest lepton or jet. Also shown is the expectation for a 140 GeV top. Two $e-\mu$ events survive the cuts, and no e-e or $\mu-\mu$ events.

The dominant backgrounds to the top dileptonic modes are expected to be from gauge boson pair production , $Z \rightarrow \tau\tau$, $b\bar{b}$ production, and lepton misidentification. The expected numbers of background events in our sample are shown in Table 7.

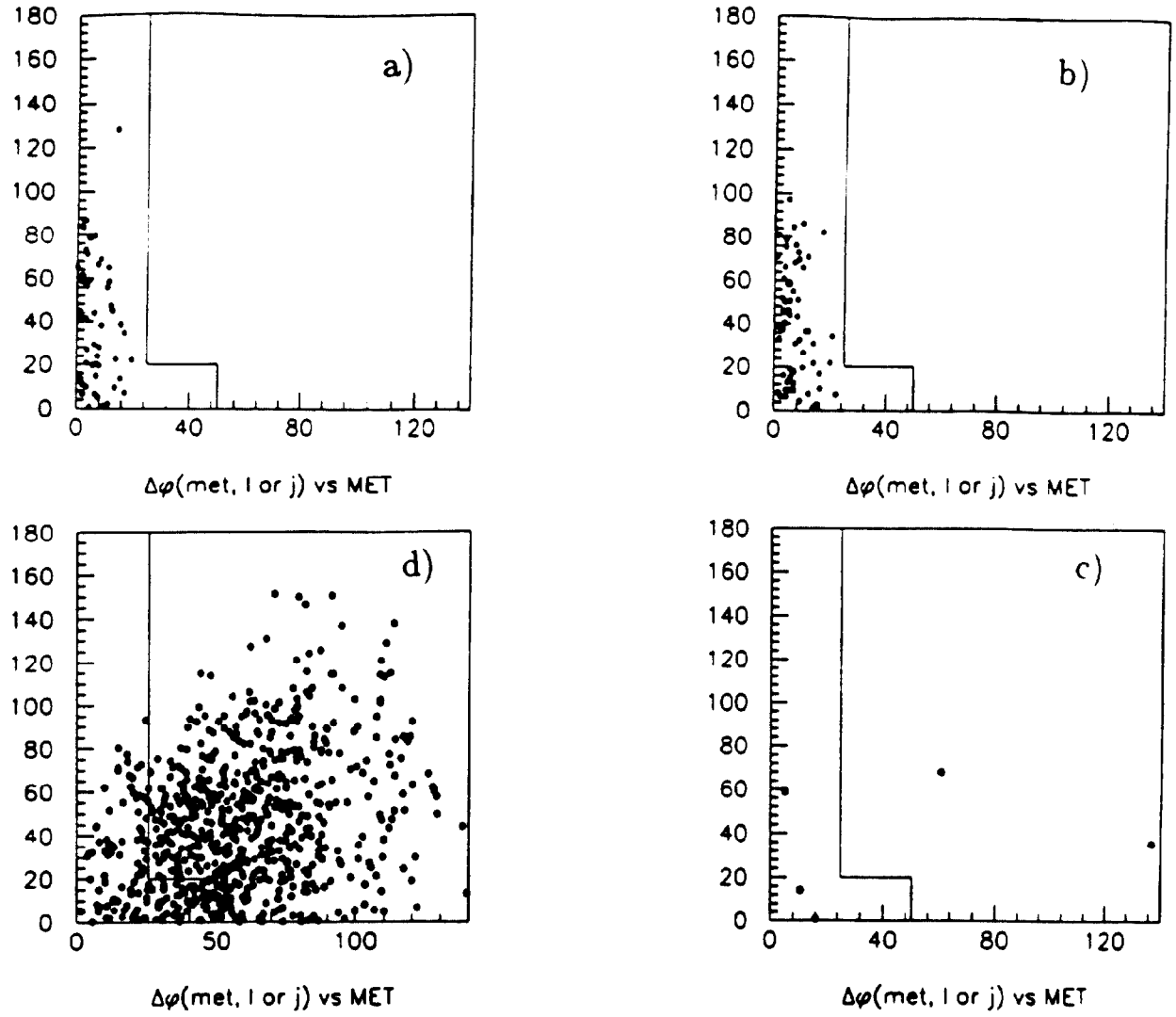

Fig.20. The distribution of events in the $\not\!\!E_T$ versus $\Delta\phi$ ($\not\!\!E_T$,jet or lepton) plane for *a)* ee and *b)* $\mu\mu$ events that survive the invariant mass cut, and *c)* $e-\mu$ events. The expected distribution for a 140 GeV top (but a much larger integrated luminosity - the total number of events expected in 21.4 pb^{-1} is 2.5) is shown in *d)*.

The characteristics of the two events are listed in Table 8. A great deal of effort has gone into understanding the kinematics etc. of these two events, but the picture remains rather unclear, which is not remarkable given only two events.

From this measurement one can extract a limit on the top production cross-section. This is underway for the cuts described above; Figure 21 shows the result as of the Lepton-Photon conference[30]. Using the lower limit on the LO cross-section from Ellis *et al.* the mass limit obtained was 113 GeV/c^2. The mass limit, however, depends on the theoretical cross-section used, while the cross-section limit is the measured number. Using the higher cross-section of the NLO calculation will result in a higher limit (see Fig.12).

Table 7: Results of the Dilepton Top analysis

		Number of events for 21.4 pb^{-1}
$e\mu$	WW	0.10 ± 0.04
	$Z \rightarrow \tau\tau$	0.07 ± 0.02
	$b\bar{b}$	0.04 ± 0.02
	Fake lepton	0.03 ± 0.03
Total Background		0.23 ± 0.05
Observed Events		2
ee, $\mu\mu$	WW	0.06 ± 0.02
	$Z \rightarrow \tau\tau$	0.06 ± 0.02
	Drell Yan	0.10 ± 0.10
	$b\bar{b}$	0.05 ± 0.03
	Fake lepton	0.04 ± 0.03
Total Background		0.32 ± 0.11
Observed Events		0

Table 8: Characteristics of the Two Dilepton Events

	Event I				Event II			
	Charge	P_T (GeV/c)	η	ϕ (deg)	Charge	P_T (GeV/c)	η	ϕ (deg)
electron	−	22.2	0.84	34	+	50.6	0.93	23
muon	+	47.7	0.17	11	−	37.3	−0.74	6
muon	+	8.8	0.18	355				
Jet 1		127.5	0.11	355		78.3	0.64	218
Jet 2		53.0	−0.54	218		15.6	−3.31	344
Jet 3		20.2	−2.94	115		14.4	1.34	344
Missing E_T		136.4		178		59.6		149
$\Delta\phi$ ($\not\!\!E_T$,ℓ)				147				124
$\Delta\phi$ ($\not\!\!E_T$,j)				36				68

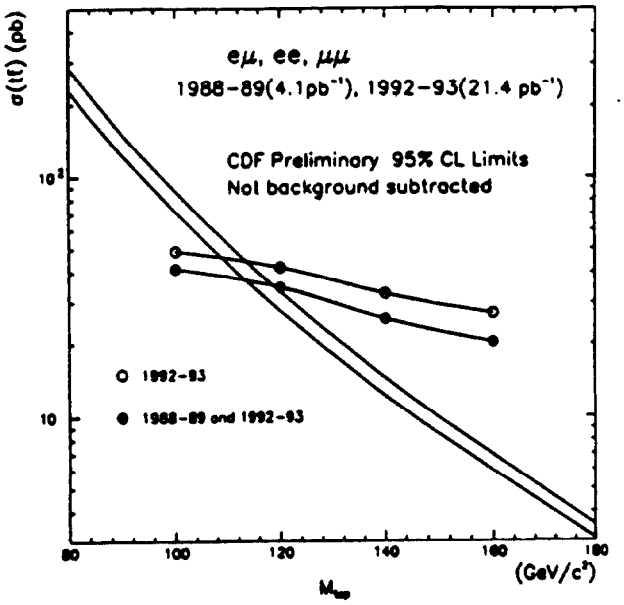

Fig.21. The limit as of the Lepton-Photon conference on the top production cross-section from the dilepton analysis.

6.2 The Lepton + Jets Analysis

This analysis searches for the case when one W decays leptonically ($e\nu, \mu\nu$), and the other hadronically ($c\bar{s}, u\bar{d}$). The resulting signature from the 2 W's and the 2 b's is thus 4 jets, of which 2 are b's, at least one high p_T lepton, and missing E_T. The kinematic distributions expected for a 160 GeV top are shown in Figure 22. Note that the p_T and $\not\!\!E_T$ observed are characteristic of W decays, and do not change rapidly with M_T. In contrast P_T^B is a 'vernier' on $M_T - M_W$, and is quite sensitive to M_T.

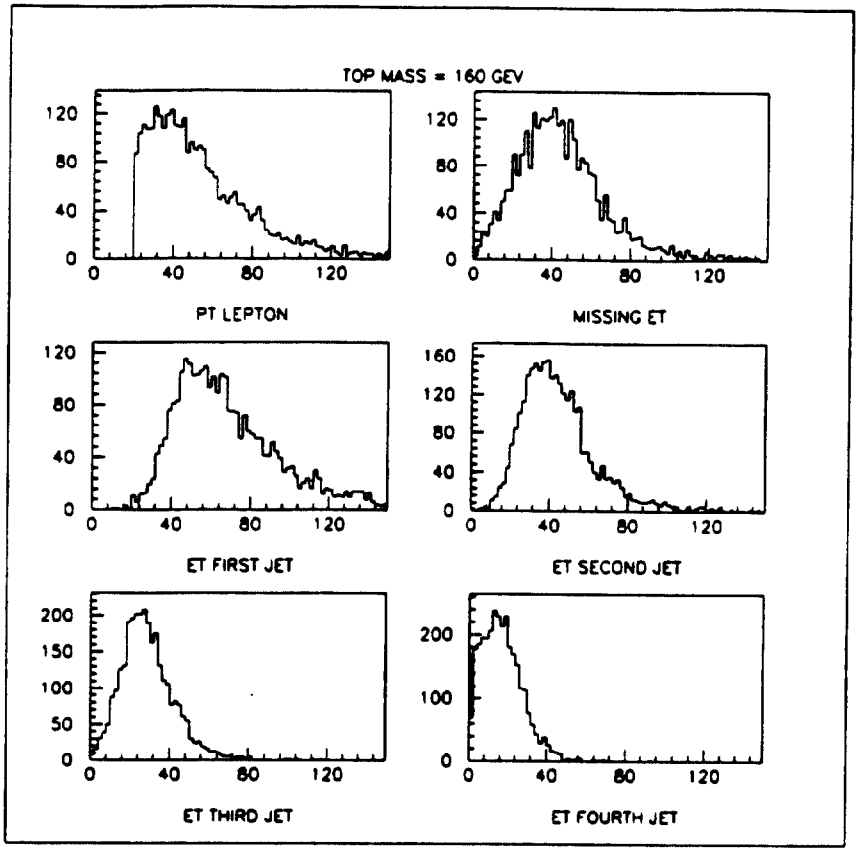

Fig.22. The predicted distributions of the lepton p_T, missing E_T, and the jet E_T distributions from the decay of 160 GeV top quarks.

I will concentrate on the analysis up to the tagging of the b's. As in the dilepton analysis, the cuts and event selection described here are new, and differ somewhat from the earlier analysis presented at the Lepton Photon Conference [30], particularly in the inclusion of the CMX muon extension system. The quotable results, however, have not changed since then, and will be presented here.

The lepton selection cuts are described in Table 9 (the variables are the same as described in Table 6). Both electrons and muons are required to be in the central detector, and to be isolated. Events with a second electron or muon (with looser cuts) which forms a pair with invariant mass in the range $70\ GeV/c^2 < M_{ll} < 110\ GeV/c^2$ are eliminated. In addition, events where the electron is flagged as coming from a photon conversion are removed. We then ask that the missing E_T, corrected in muon events for the primary muon, and in all events for muons with p_T greater than 10 GeV/c, be greater than 20 GeV. Finally,

runs where some part of the detector was not functioning well were removed, and the events were required to have satisfied the appropriate triggers at Levels 1, 2, and 3. The numbers of events passing these cuts (with conversions already removed from the electrons) are given in Table 10. About 9000 events are removed by the conversion filter.

Table 9: Cuts for the electron and muon lepton categories (see the glossary for the dilepton event selection).

Central Electrons			Central and Extension Muons		
E_t	$>$	20 *GeV*	P_t	$>$	20 *GeV/c*
E/p	$<$	1.5	EM	$<$	2 *GeV*
Had/EM	$<$	0.05	HAD	$<$	6 *GeV*
$Lshr$	$<$	0.2			
Δx	$<$	1.5 cm	$\Delta x(CMU)$	$<$	5 cm
Δz	$<$	3.0 cm	$\Delta x(CMUP)$	$<$	5 cm
$\chi^2(strip)$	$<$	15	$\Delta x(CMUX)$	$<$	10 cm
d_0	$<$	3 mm	d_0	$<$	3 mm
Δz_{vert}	$<$	5 cm	Δz_{vert}	$<$	5 cm
$\|Z_{vert}\|$	$<$	60 cm	$\|Z_{vert}\|$	$<$	60 cm
$Isol.$	$<$	0.1	$Isol.$	$<$	0.1

The problem with this mode is that there is a substantial and insidious background from the production of a W boson with accompanying jets. The signature of lepton, missing E_T, and jets, is nominally the same as the signal. Against the background we have two handles: possible topological differences between top and W+jets, and the fact that in top events two of the jets are b's. A great deal of effort is going into investigating the rejection power of these two handles; the word is not in yet on how much power is in them, and on what we see for sure.

Table 10: Cuts and event numbers for the electron and muon lepton categories, before b-tagging.

Selection Description	Electron	Muons
Good lepton	28,522	17,994
Isolation Cut	20,420	11,901
Z's Removed	18,701	11,394
$\not\!\!E_T > 20$ *GeV*	13,658	8,725
Bad runs removed	12,798	8,273
Trigger required	11,949	7,023
With Jets of $E_T > 15$ *GeV* and $\|\eta\| < 2.0$		
0 Jets	10,663	6,264
1 Jet	1058	655
2 Jets	191	90
3 Jets	30	13
$\geq$ 4 Jets	7	2

Table 11: Number of events expected in the electron and muon lepton +jets samples in an integrated luminosity of 21.4 pb^{-1} before 'b-tagging'. The rows are the numbers expected or observed in events with 1,2, 3, or 4 jets. The 'W+njet' columns are the predicted backgrounds due to the W+jet QCD/Electroweak background, and are from Vecbos: only the diagonal elements (in bold) are to be used. The columns labelled 'Top' are predictions from Isajet for top masses of 100,120, and 140 GeV. The column labelled data gives the observed number of events in that category. The statistical uncertainties in the Monte Carlo numbers are of order 10%.

Topology	Expected W+Jets Background				Expected Signal				-Data-
	W+1jet	W+2jets	W+3jets	W+4jets	Top 100	Top 120	Top 140	Top 160	Top 180	
Electrons, Missing Et, and Jets										
e+$\not\!\!E_T$+ 1 jet	**937**	**618**	**342**	**115**	**31**	**6.0**	**1.7**	**0.5**	**0.2**	**1058**
e+$\not\!\!E_T$+ 2 jets	**16**	**89**	**146**	**78**	**38**	**13**	**5.1**	**2.1**	**0.9**	**191**
e+$\not\!\!E_T$+ 3 jets	**0**	**6**	**29**	**34**	**22**	**14**	**7.1**	**3.4**	**1.6**	**30**
e+$\not\!\!E_T$+≥4 jets	**0**	**2.4**	**0.9**	**5.8**	**12**	**11**	**6.6**	**4.3**	**2.4**	**7**
Muons, Missing Et, and Jets										
μ+$\not\!\!E_T$+ 1 jet	**585**	**402**	**224**	**68**	**19**	**4.7**	**0.9**	**0.4**	**0.1**	**655**
μ+$\not\!\!E_T$+ 2 jets	**4.1**	**91**	**105**	**59**	**26**	**8.8**	**3.6**	**1.5**	**0.7**	**90**
μ+$\not\!\!E_T$+ 3 jets	**4.1**	**2.4**	**15**	**21**	**16**	**9.6**	**5.4**	**2.5**	**1.3**	**13**
μ+$\not\!\!E_T$+≥4 jets	**0.**	**0.**	**0.9**	**3.0**	**10**	**8.6**	**5.4**	**3.3**	**2.1**	**2**
Total Lepton, Missing Et, and Jets										
l+$\not\!\!E_T$+ 1 jet	**1522**	**1020**	**566**	**183**	**50**	**11**	**2.6**	**0.9**	**0.3**	**1713**
l+$\not\!\!E_T$+ 2 jets	**20**	**180**	**251**	**137**	**64**	**22**	**8.7**	**3.6**	**1.6**	**281**
l+$\not\!\!E_T$+ 3 jets	**0.**	**8.4**	**44**	**55**	**38**	**24**	**13**	**5.9**	**2.9**	**43**
l+$\not\!\!E_T$+≥4 jets	**0.**	**2.4**	**1.8**	**8.8**	**22**	**20**	**12**	**7.6**	**4.5**	**9**

The expected event rates for various top masses, the numbers of background events expected from W+jets as calculated using the Vecbos program [28], and the number of events observed, as a function of the number of jets, are shown in Table 11. For the W+jet estimates, only the numbers on the diagonal (in bold) are physical; the off-diagonal elements are expected to be mostly artifacts of the generation process. The Monte Carlo estimates have a statistical uncertainty of approximately 10%, and a large systematic uncertainty.

The table is instructive- for a 140 GeV top one sees that the signal is approximately equal to the background at the 10 event level in the W+4 jets bin. For the W+3 jets bin, the statistics is about the same for a 140 GeV top (for example), but the background is four times worse. With a method with a large rejection against background but a relatively low efficiency, such as b-tagging, it pays to sum the W+3 jet and W+4 jet channels to get the factor of approximately two in signal acceptance.

For example, a 160 GeV top is expected to result in 13.5 events detected in the sum of the two bins. With a b-tagging efficiency per event of 30%,say, one would expect to have 4 events with at least one tagged b. The total background before b-tagging from the table is about 53 events: to get an expected background below 0.5 events, again for example, one needs a rejection factor of 100:1.

For the lepton + $\not\!\!E_T$ +4 jet events one should use a method with lower rejection, but higher efficiency. The b- tagging could presumably be tuned for this. In addition these characteristics are more typical of the topological analyses. Eventually we hope to be able to use all of the information in a way that maximizes the signal-to-noise, and yet is not heavily dependent on Monte Carlo expectations.

For illustration, I have taken the Monte Carlo expected signal and W+jet background numbers from Table 11 for both a 140 GeV and 160 GeV top, and calculated the expected number of events S, the expected number of background W+ jet events B, and the significance $S^2/(S+B)$, for a range of rejection factors and for a range of efficiencies for an unspecified algorithm to distinguish top events from W+jet events. These are presented in Table 12. They should be taken with many grains of salt, but are educational of the effects of the two problems of small statistics and of signal-to-noise on the strategy, and on the present expected reach in mass.

6.2.1 Separating W+jet and Top events: b-tagging

Top events will differ from W+jet background events in topology, and also in that 2 of the 4 jets are the b quarks from the top primary decay ("b-jets"). Both topological and "b-tagging" background rejection algorithms are being worked on. The b-tagging is powerful in that it not only rejects background but also adds important kinematic information- which jet is a b. We will use all the information we can. The description below, however, is of the 'snapshot' of the analysis as of July-October 1993, and will be superceded as we understand the tagging, topology, and backgrounds better. I was consequently brief about the tagging- for a fuller description of the details of the tagging during this time period the reader is referred to the expert talks of Contreras [29] and Tipton [30]. The numbers in the previous section on the event selection before 'b-tagging' should stand up into the new analyses, however.

Table 12: The number of Monte Carlo signal events (S), W+jet background events (B), and the significance ($\sigma = (S^2/(S+B))$ after applying any algorithm of a given rejection factor (the rows) and given efficiency (the columns), for top masses of 140 and 160 GeV. The numbers are derived from the Monte Carlo expectations for 21.4 pb^{-1} listed in Table 11, and have statistical uncertainties of 10%. More importantly, they are Monte Carlo, and should be treated with appropriate scepticism.

	Top Identification Efficiency														
	10%			30%			50%			70%			90%		
Rej.	S	B	σ	S	B	σ	S	B	σ	S	B	σ	S	B	σ
140 GeV Top; W + ≥ 3 Jets															
300	2.5	0.2	2.3	7.5	0.2	7.3	12.5	0.2	12.3	17.5	0.2	17.3	22.5	0.2	22.3
100	2.5	0.5	2.1	7.5	0.5	7.0	12.5	0.5	12.0	17.5	0.5	17.0	22.5	0.5	22.0
30	2.5	1.7	1.5	7.5	1.7	6.1	12.5	1.7	11.0	17.5	1.7	15.9	22.5	1.7	20.9
10	2.5	5.2	0.8	7.5	5.2	4.4	12.5	5.2	8.8	17.5	5.2	13.5	22.5	5.2	18.2
3	2.5	17.5	0.3	7.5	17.5	2.3	12.5	17.5	5.2	17.5	17.5	8.8	22.5	17.5	12.7
140 GeV Top; W + ≥ 4 Jets															
300	1.2	0.0	1.2	3.6	0.0	3.6	6.0	0.0	6.0	8.4	0.0	8.4	10.8	0.0	10.8
100	1.2	0.1	1.1	3.6	0.1	3.5	6.0	0.1	5.9	8.4	0.1	8.3	10.8	0.1	10.7
30	1.2	0.3	1.0	3.6	0.3	3.3	6.0	0.3	5.7	8.4	0.3	8.1	10.8	0.3	10.5
10	1.2	0.9	0.7	3.6	0.9	2.9	6.0	0.9	5.2	8.4	0.9	7.6	10.8	0.9	10.0
3	1.2	2.9	0.3	3.6	2.9	2.0	6.0	2.9	4.0	8.4	2.9	6.2	10.8	2.9	8.5
160 GeV Top; W + ≥ 3 Jets															
300	1.4	0.2	1.2	4.1	0.2	3.9	6.8	0.2	6.6	9.4	0.2	9.3	12.1	0.2	12.0
100	1.4	0.5	1.0	4.1	0.5	3.6	6.8	0.5	6.3	9.4	0.5	9.0	12.1	0.5	11.6
30	1.4	1.7	0.6	4.1	1.7	2.8	6.8	1.7	5.4	9.4	1.7	8.0	12.1	1.7	10.6
10	1.4	5.2	0.3	4.1	5.2	1.8	6.8	5.2	3.8	9.4	5.2	6.1	12.1	5.2	8.5
3	1.4	17.5	0.1	4.1	17.5	0.8	6.8	17.5	1.9	9.4	17.5	3.3	12.1	17.5	5.0
160 GeV Top; W + ≥ 4 Jets															
300	0.8	0.0	0.7	2.3	0.0	2.3	3.8	0.0	3.8	5.3	0.0	5.3	6.8	0.0	6.8
100	0.8	0.1	0.7	2.3	0.1	2.2	3.8	0.1	3.7	5.3	0.1	5.2	6.8	0.1	6.8
30	0.8	0.3	0.5	2.3	0.3	2.0	3.8	0.3	3.5	5.3	0.3	5.0	6.8	0.3	6.6
10	0.8	0.9	0.4	2.3	0.9	1.6	3.8	0.9	3.1	5.3	0.9	4.6	6.8	0.9	6.1
3	0.8	2.9	0.2	2.3	2.9	1.0	3.8	2.9	2.1	5.3	2.9	3.4	6.8	2.9	4.8

6.2.2 Displaced Vertex b-tagging

The Silicon Vertex Detector (SVX) is a 4-layer tracking device made of single-layer silicon strip detectors positioned at radii between 3.0 and 7.9 cm from the beamline. The inner three layers have 60 μm strips; the outer layer has 55 μm strips. The device is made in two halves, each 25.55 cm. long, with a gap between them of 3.485 cm. The luminous region is in fact longer than the SVX, with a typical σ of $\approx$ 25 cm ($\approx$ 30 cm averaged over the whole run).

The tagging is done by starting with the jets in the calorimeter with $E_T > 15\ GeV$, $|\eta| < 2$, and at least 2 good tracks in the CTC that match a good track in the SVX. We expect from Monte Carlo that $\approx 2/3$ of 140 GeV top events will have 3 or more jets that satisfy the the jet calorimeter requirements. Approximately 60% of 140 GeV top events are expected to have at least one b-jet that has at least two tracks of $p_T > 2$ GeV in the fiducial volume of the SVX.

The actual tagging efficiency is measured by comparing tagging rates in an inclusive low-pt electron sample (estimated to be $\approx$ 40% semileptonic b decay) with an ISAJET $b\bar{b} \rightarrow e^+e^- + X$ sample. Both the rate of single-tags and the ratio of double-tags to single tags are measured and compared to Monte Carlo predictions. The Monte Carlo predictions for this b sample are found to be too high by a factor of 0.75 ± 0.25. This factor is then applied to the tagging rate for b's from top in the Monte Carlo. Work is going on to better understand this: the SVX data have not yet been corrected for a gradual diminishing of the signal-to-noise due to radiation damage during the run, for example.

Including this correction factor, we find that approximately 22% ($\pm$5%) of top events will have at least one b tagged by the SVX, for top masses in the range 140-160 GeV. In 21.4 pb^{-1} we expect 5$\pm$2 SVX-tagged events for a 140 GeV top, and 2.3 ± 0.9 for a 160 GeV top.

The background estimates are crucial [31]. Backgrounds are expected to be : 1) $Wb\bar{b}$ and $Wc\bar{c}$ production [32], 2) false tags due to pattern recognition confusion in the tracking, 3) Wc production, 4) $b\bar{b}$ production, 5) WW and WZ pairs, and 6) $Z \rightarrow \tau\tau$. The first two backgrounds, which turn out to be the largest, are estimated by two different methods, one which puts an upper limit on the sum of the effects directly from a control sample, and the other which uses Monte Carlo to estimate the $Wb\bar{b}$ and $Wc\bar{c}$ contributions which is then added to a measurement of the false tag rate. Method 1 ('the generic jet assumption') uses a large control sample of jets that pass a 50 GeV trigger to assign a probability per jet of being tagged as a function of the Et and track multiplicity of the jet. These probabilities are then applied to each jet in the W+jets sample to estimate the background. The assumption is that the false tag rates will be estimated correctly this way, and any contribution from real heavy flavor in jets is likely to be overestimated, as there are direct $b\bar{b}$ and $c\bar{c}$ contributions to the control sample, while the jets in the W+jets sample are more dominated by gluons. In addition we assume that there are no correlations that increase the tagging rate as a function of the number of jets. Method 2 uses the 'negative decay length tags' to estimate the false tag rate, and calculates $Wb\bar{b}$ and $Wc\bar{c}$ explicitly using the Herwig Monte Carlo program and the leading order matrix elements [32]. This method also assumes no dependence of the tagging rate as a function of the number of jets.

The third background in our list, Wc production, is determined from the Vecbos and Herwig Monte Carlos [33]. The fourth, $b\bar{b}$ production, is determined directly from the data by extrapolating in the $\not\!\!E_T - Iso$ plane [34]. Finally, WW, WZ, and $Z \rightarrow \tau\tau$ backgrounds are estimated from ISAJET. These estimates are then added to the estimates of the heavy flavor and mistags from either Method 1 or Method 2 above to give the total estimates which are presented in Table 13. Please note that these numbers are as of the Lepton-Photon Conference and will change.

Events tagged in $\int \mathcal{L}dt$=21.4 $\pm$ 2.1 pb^{-1}	$N_{jets} = 1$	$N_{jets} = 2$	$N_{jets} \geq 3$
Data	3	6	3
Background Method 1	7.0 $\pm$ 1.7	2.4 $\pm$ 0.5	1.0 $\pm$ 0.2
Background Method 2	5.8 $\pm$ 1.7	1.5 $\pm$ 0.5	0.58 $\pm$ 0.25
M_t = 140 GeV/c^2	0.5 $\pm$ 0.2	1.8 $\pm$ 0.7	4.7 $\pm$ 1.8

Table 13: Summary of SVX Tagging Analysis

The number of events observed after tagging in the 1, 2, 3, and $\geq$4 jet bins is shown in Figure 23. The backgrounds as estimated by Methods 1 and 2 are also shown.

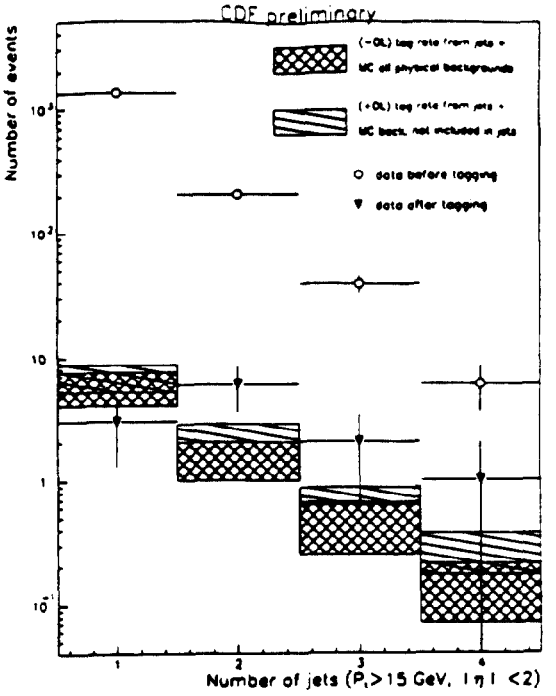

Fig.23. A preliminary plot of the number of tagged events versus the number of jets in events in the SVX lepton + jets analysis sample. The background estimates from both Methods 1 and 2 are shown.

6.2.3 Soft lepton b-tagging

An alternative method of tagging b quarks is by identifying low- momentum (soft) leptons near jets. Each of the two b's decays sequentially, resulting in 2 chances each to make a soft lepton, with a branching ratio each time of about 10%. In addition, the W that decays hadronically half the time goes to $c\bar{s}$, giving another 10% chance for a lepton (although also a chance for confusion as to which is the b jet). The efficiency for finding electrons down to p_T of 2 GeV is determined from a sample of photon conversions where one leg is identified as an electron and the other tests the efficiency of the algorithm. The effect of nearby energy is calculated by Monte Carlo. Muons with p_T down to 2 GeV are also used, with the efficiencies determined from a large sample of $J/\psi \rightarrow \mu\mu$ decays. As of the time of the talk there were not yet results available: however the tagging efficiency of this method is very comparable to, and uncorrelated with, that of the SVX method described above.

6.3 Summary

The top search analysis is developing rapidly, as we learn how to identify b jets and learn more about the backgrounds. For top masses above 120 GeV or so the dilepton mode, with a branching ratio of 4/81, is limited in statistics (although tagging the b jets in dilepton events reduces the background to almost nothing). In the lepton + jets mode, for which the branching ratio is 24/81, the b jet identification is necessary, and looks extremely promising.

There are also strong topological constraints on the top decays; an analysis that combines a mature b-tagging with the topological information will be powerful. The acceptances for the dilepton and SVX lepton+jets analyses are given in Table 14.

Top-quark Mass	120 GeV/c^2	140 GeV/c^2	160 GeV/c^2	180 GeV/c^2
$\sigma_{t\bar{t}}(pb)$	35.3	15.6	7.7	4.0
ϵ_{SVX}	$1.0 \pm 0.2\%$	$1.4 \pm 0.3\%$	$1.5 \pm 0.3\%$	$1.6 \pm 0.4\%$
$\epsilon_{Dilepton}$	$0.48 \pm 0.07\%$	$0.65 \pm 0.09\%$	$0.76 \pm 0.11\%$	$0.84 \pm 0.13\%$

Table 14: Summary of Top Acceptance and Tagging Efficiency

A summary of the number of events expected for different top masses, and the preliminary numbers on expected backgrounds and on observed events is shown in Table 15. The dilepton analysis numbers have been updated since the Lepton-Photon Conference; the SVX analysis numbers are the same as then.

Channel	SVX	Dilepton
Expected # events $M_t = 120$ GeV/c^2	7.3 ± 2.7	3.7 ± 0.6
Expected # events $M_t = 140$ GeV/c^2	4.7 ± 1.8	2.2 ± 0.3
Expected # events $M_t = 160$ GeV/c^2	2.3 ± 0.9	1.3 ± 0.2
Expected # events $M_t = 180$ GeV/c^2	1.5 ± 0.6	0.7 ± 0.1
Expected Background	1.0 ± 0.2	0.55 ± 0.13
Observed Events	3	2

Table 15: Summary of Expected Signal Events and Backgrounds for 21.4 pb^{-1}.

7 Prospects, Summary, and Conclusions.

The Tevatron Collider Run that ended May 30 (Run Ia) netted CDF an integrated luminosity of 21.4 pb^{-1}, a factor of almost 5 over the 1988-89 run. Run Ib is scheduled to begin this fall, with another factor of 3-4 expected (the new linac will increase the luminosity).

For Electroweak physics, CDF has accumulated approximately 10,000 $W^{\pm} \rightarrow e^{\pm}\nu$, 1000 $Z^0 \rightarrow e^+e^-$, 7000 $W^{\pm} \rightarrow \mu^{\pm}\nu$, and 500 $Z^0 \rightarrow \mu^+\mu^-$ events in this last run. Precision measurements that are unique to the Tevatron, such as measurements of the W width and mass, are underway. Gauge boson pair production is observed, and is being studied. Limits on new gauge bosons are at the 0.5 TeV level. These searches and measurements in the 0.5-1 TeV region are just beginning as we accumulate larger and larger integrated luminosity. Finally, the search for the top quark has shown us that the top quark is exceptionally heavy, perhaps a hint of something beyond. The top search is in full swing, with emphasis on identification of the b quarks from top decay and on the topology of the events.

The future physics at the Collider looks promising. The Tevatron will remain the highest energy machine in the world for at least a decade. With the Main Injector data sets in the 10 fb^{-1} or greater may be possible. Even scaling from our present detection efficiencies (which can be improved), 10 fb^{-1} would provide a sample of 650 detected top dilepton decays, with approximately 200 with a tagged b jet. The tagged lepton+jets samples would be factors of 2-3 larger. For at least a decade this is our window on the top and, hopefully, the physics beyond it that makes the top so heavy.

8 Acknowledgements

I would like to thank my many CDF colleagues who worked so hard in the last run. Special thanks are due to Sacha Kopp and Greg Sullivan for providing figures for the R analysis in electrons, Mark Dickson for figures for the forward/backward W asymmetry, Steve Errede for the $W\gamma$ numbers, David Saltzberg for the W mass analysis, and Sarah Eno and Jimmy Proudfoot for their efforts as excellent CDF electroweak convenors. Special thanks for putting up with my stupid questions on the top analyses are due to (at least) Dan Amidei, Claudio Campagnari, Milciades Contreras, Lina Galtieri, Soo Bong Kim, Tony Liss, Michelangelo Mangano, Mel Shochet, Paul Tipton, Gordon Watts, and Brian Winer. I thank Eric Laenen for providing the figures on top production, and Jon Rosner and James Stirling for sharing their wisdom. Lastly, I thank Marty Block and Alan White for a really pleasant conference of good physics and good company.

References

[1] The luminosity numbers quoted here have an uncertainty of approximately 10%.
[2] For a more detailed presentation of the electroweak results see T. Muller, Proc. Int. Europhysics Conf. on High Energy Physics, Marseille, July 22 - 28, 1993, and also H.J. Frisch, proceedings of the Blois Vth Workshop, Brown University, June 7-12, 1993, H. Fried, K. Kang and C-I Tan, eds., to be published.
[3] N. Cabibbo, Third Topical Workshop on Proton-Antiproton Collider Physics, Rome, 1983, pp. 567-569.
[4] F. Halzen and M. Mursula, Phys. Rev. Lett. 51, 857 (1983).
[5] CDF Collaboration, F. Abe *et al.*, Phys. Rev. D44, 29 (1991), Phys. Rev. Lett. 64, 152 (1990).
[6] The E/p cut has been changed [see Ref. 5] from $E/p < 1.5$ to $0.5 < E/p < 2.0$, and the cut on the chisquared on the shower maximum (strip) chamber has been changed from 15 to 10.
[7] The central electromagnetic calorimeter fiducial region covers a rapidity range from 0 to 1.0, the plug from 1.1 to 2.4, and the forward calorimeter from 2.4 to 4.2.
[8] J. Rosner, M. Worah, and T. Takeuchi, Univ. of Chicago preprint EFI 93-40, Aug. 1993; Phys. Rev. D49, (1994), to be published.
[9] CDF Collaboration, F. Abe et. al, Phys. Rev. Lett. 69, 128 (1991).
[10] See, for example, F. Halzen and S. Keller, in Proceedings of the Workshop on Hadron Structure Functions and Parton Distributions, FNAL, April 1990, D. Geesaman, J. Morfin, C. Sazama, and W. K. Tung, eds. (World Scientific).
[11] UA2 Collaboration; J. Alitti *et al.*, Phys. Lett. B276, 354 (1992).

[12] CDF Collaboration, F. Abe *et al.*, Phys. Rev. Lett. 65, 2243 (1990), Phys. Rev. D43, 2070 (1991).
[13] David Saltzberg, presented at the 9th Topical Workshop on Proton-antiproton Collider Physics, Tsukuba, Japan, October 1993. The preliminary number from the electron mode alone is $M_W = 80.47 \pm 0.15(stat) \pm 0.25(sys)$. The uncertainty may get smaller as the analysis matures.
[14] Srini Rajogopalan, for the D0 Collaboration, proceedings of the Blois Vth Workshop, Brown University, June 7-12, 1993, H. Fried, K. Kang and C-I Tan, eds., to be published.
[15] Minutes of a LEPC meeting, spring 1993.
[16] V. Barger, T.Han, J.Ohnemus, and D.Zeppenfeld, Phys. Rev. D41, 2782. (1990)
[17] From the Jade experiment we know $A_b = T^b_{3L} - T^b_{3R} = 0.54 \pm 0.15$. See also: The CLEO Collaboration, Phys. Rev. D47, 791, 1993.
[18] W. Hollik, Proceedings of the XVI International Symposium on Lepton-Photon Interactions, August 10-15,1993, Cornell Univ., to be published.
[19] See, for example, Andrej Buras and Michaela Harlander, MPI-PAE/PTh 1/92, also to appear in the Review Volume on Heavy Flavors, eds. A.J. Buras and M. Lindner, Advanced Series on Directions in High Energy Physics, World Scientific Publishing Co., Singapore.
[20] Y. Nambu, Enrico Fermi Institute (Univ. of Chicago) preprints EFI 88-39, EFI 88-62, and in the 1988 International Workshop on New Trends in Strong Coupling Gauge Theories, Nagoya, Japan. See also, for example, W.A. Bardeen, C.T. Hill, M. Lindner, Phys. Rev. D41, 1647 (1990), and C.T. Hill, M.A. Luty, and E.M. Paschos, Phys. Rev. D43, 3011, 1991; W. A. Bardeen, C.T. Hill, FERMILAB-PUB-92-82-T, to appear in "Heavy Flavors" edited by A. Buras and M. Lindner, World Scientific.
[21] See also Hollik, *op. cit.* for a comprehensive summary.
[22] The numbers plotted are $M_T = 124^{+40+21}_{-56-21}$ (LEP data only- the value is 132^{+27+18}_{-31-19} if UA2/CDF and ν data are included), F. Merritt, Aspen 1992; $M_T = 147^{+17+17}_{-19-19}$, F. Rolandi, Dallas 1992; $M_T = 164^{+16+18}_{-17-21}$, M. Swartz, Cornell 1993 (α_s free). The Higgs mass is assumed to be 300 GeV/c^2. It reminds one of the old New Yorker cartoon (Peter Arno?) of the gas station attendant saying to the driver of a monstrous Cadillac "Sir, could you please turn it off? You're gaining on me...").
[23] After the talk was given the CDF Collaboration 'blessed' new estimates on the backgrounds for the dilepton channel. I have taken the anachronistic liberty of updating these numbers.
[24] The D0 experiment uses the central value of the NLO prediction, which is perfectly reasonable. As an experimentalist I would prefer to emphasize the cross-section limit, which is measured, to a mass limit, which is derived.
[25] R. K. Ellis, Phys. Lett. B259, 1991.
[26] E. Laenen, J. Smith, W.L. van Neerven, FERMILAB-PUB-93-270-T, Aug 1993, and E. Laenen, private communication.
[27] For electrons, see Ref. 5. For muons, see F. Abe *et al.* (CDF collaboration), Phys. Rev. Lett. 69, 28 (1992).
[28] F.A. Berends, W.T. Giele, H. Kuijf, and B. Tausk, Nucl. Phys. B357, 32 (1991).
[29] M. Contreras, invited talk at the 9th $\bar{p}p$ Workshop, Tsukuba U., Japan, October 1993.
[30] The CDF collaboration, presented by P. Tipton; Proceedings of the XVI International Symposium on Lepton-Photon Interactions, August 10-15, 1993, Cornell Univ., to be published.
[31] See, for example, UA1 Collaboration, Phys. Lett. 147B, 493, 1984.
[32] M. L. Mangano, Nucl. Phys. B405, 536 (1993).
[33] See U. Baur, F. Halzen, S. Keller, M. L. Mangano, and K. Riesselmann, FSU-HEP-930815 preprint, August 1993, for a description of the physical processes.
[34] This method is explained in F. Abe *et al.*, Phys. Rev. D44,29 (1991).